Transfer Learning for Angle of Arrivals Estimation in Massive MIMO System

Zhiheng Guo*, Kuijie Lin*, Xiang Chen*‡ and Chong-Yung Chi†
*School of Electronics and Information Technology, Sun Yat-sen University, Guangzhou, China
†Department of Electrical Engineering, Institute of Communications Engineering, NTHU, Hsinchu 30013, Taiwan
Email:{guozhh7, linkj25}@mail2.sysu.edu.cn, chenxiang@mail.sysu.edu.cn, cychi@ee.nthu.edu.tw

2022 IEEE/CIC International Conference on Communications in China (ICCC) | 978-1-6654-8480-0/22/$31.00 ©2022 IEEE | DOI: 10.1109/ICCC55456.2022.9880615

***Abstract*—Angle-of-arrivals (AoAs) estimation is one of the key tasks of localization in massive multiple-input-multiple-output (MIMO) system. Among all AoAs estimation methods, the class of deep learning (DL) based methods has been recognized effective with high estimation accuracy and low complexity. However, the design for methods in this class requires obtaining adequate labeled training data and training a specific network for each of different channels in MIMO system, which is challenging and costly. To overcome this bottleneck, a transfer learning method is proposed in this paper based on the assumption that some common features exist among different channel models. The proposed method is implemented by a deep residual network (ResNet) composed of transfer layers (to extract the common features) followed by fine-tuning layers (to extract other characteristic features) in cascade, thus without need of a specific network for each different channel. As a realization of the proposed framework, the ResNet is trained on the data from the source domain (i.e. the "basic" channel model) to obtain the weights of transfer layers (fixed thereafter), which are used to initialize the fine-tuning layers. Then, small amounts of data from the target domain (i.e., a more sophisticated channel model like spatial channel model), are used to adjust the weights of fine-tuning layers. Finally, extensive simulation results demonstrate that the AoAs estimation accuracy of the proposed method is comparable to that of supervised DL-based methods, for which a specific trained network is required for each channel.**

***Index Terms*—Angle of Arrival, Massive MIMO, Deep Learning, Transfer Learning, Spatial Channel Model.**

I. Introduction

Massive multiple-input-multiple-output (MIMO) is one of the vital technologies in fifth generation (5G) and beyond wireless communication systems. As a key task of localization in any massive MIMO system, angle-of-arrivals (AoAs) estimation has aroused great attention in the past decades. However, there are still challenges in accurate AoAs estimation, arising from sophisticated channel modeling, high computational complexity due to a large number of antennas applied, etc.

The classic methods for AoAs estimation in MIMO system are subspace-based estimation methods, dating back to some classic algorithms such as MUltiple SIgnal Classification (MUSIC) [1] and Estimation of Signal Parameters via Rotational Invariant Techniques (ESPRIT) [2]. In recent years, some further development of subspace-based methods emerged, such as the algorithms with special antenna array configurations [3], methods used in millimeter wave massive MIMO (mmMIMO) system [4], etc. However, due to the eigendecomposition of high-dimensional channel covariance matrices in massive MIMO system, they may suffer from high computational complexity.

Another class of methods based on compressed sensing (CS) was proposed to reduce the computational complexity. Such methods usually formulate the AoAs estimation as optimization problems, then reformulate them into semi-definite programs, and then solve them by interior-point method. Some excellent works have been proposed by using the alternating direction method of multipliers [5], and some have been extended to arbitrary antenna array [6]. However, these methods are based on some strict assumptions on the sparsity of the wireless channels and/or the structure of the received signals, so making it hard applied to more general channel models.

The recent development of machine learning has spurred the applications of deep learning (DL) to AoAs estimation. In general, DL-based methods can be categorized into "data-driven" methods [7] and "model-driven" methods [8]. The former follows the end-to-end principle and trains the networks on a large number of labeled training data [9]. In contrast, model-driven methods exploit the established physical models and properties of signal propagation in wireless channel, such as combining the DL with the subspace-based methods [10], applying DL to CS-based algorithm [11], etc. Compared with other classic methods, DL-based methods shift main computation tasks to the training stage for low complexity during deployment. However, it must train a specific network for each channel scenario (or proper channel model) which is costly and impractical with limited labeled training data.

To our best knowledge, our work is the first by combining transfer learning with AoAs estimation across various channel models in massive MIMO system. Similar to DL-based methods, our framework has low computational complexity during deployment, and can be applied to more general scenarios. Based on the key assumption that channel models used for AoAs estimation in different scenarios share some common features, the proposed framework requires only one network (transfer layers), followed by fine-tuning layers for AoAs estimation, and hence overcomes the above-mentioned bottleneck

‡ Xiang Chen is the corresponding author.

This work was supported partly by the State's Key Project of Research and Development Plan under Grant 2019YFE0196400, and partly by the Ministry of Science and Technology, Taiwan, under Grants MOST 111-2221-E-007-035-MY2 and MOST 110-2221-E-007-031.

issue of the DL-based methods. Compared with the existing transfer learning works used in wireless communications [12], the channel models in the source domain are different from those in the target domain. Specifically, the framework is trained by the data from a "basic" simulation channel model in the source domain, while the final estimation is made on a sophisticated channel from the protocol, i.e., spatial channel model (SCM) [13].

II. SYSTEM MODEL

In this paper, two different channel types in massive MIMO uplink systems are considered as source and target domain, respectively. For the source domain, a "basic" channel is modeled which consists of one base station (BS) and K mobile stations (MSs). The BS is equipped with a uniform linear array (ULA) of N_r antenna elements, and each MS equipment has one antenna. The MSs are assumed to be stationary (zero mobile speed) for T time slots, during which the BS collects T snapshots of the received signals to estimate the MSs' locations. Each MS k's location is specified by the distance to the BS and the AoA $\theta_k \in [-\frac{\pi}{2}, \frac{\pi}{2}]$. MS k's AoA θ_k is the impinging direction of the received signal, relative to the broadside of the BS's antenna array (i.e., perpendicular to the antenna array). Given the AoA θ_k, MS k's signal experiences different phase shifts across the antenna array, as characterized by the array response vector

$$\boldsymbol{a}(\theta_k) = \left[1, e^{j\frac{2\pi d_s}{\lambda}\sin\theta_k}, \ldots, e^{j\frac{2\pi d_s}{\lambda}(N_r-1)\sin\theta_k}\right]^T, \quad (1)$$

where λ is the wavelength and $d_s \geq \frac{\lambda}{2}$ is the inter-element distance (in meters) of BS antenna array.

MS k's signal is also attenuated due to the slow fading channel in the source domain. The vector of channel gains from the K MSs to the BS is denoted by $\boldsymbol{h} = \boldsymbol{\alpha} \odot e^{j\boldsymbol{\psi}}$, where "$\odot$" denotes the component-wise product of two vectors with the same dimension, $\boldsymbol{\alpha} = [\alpha_1, \alpha_2, \ldots, \alpha_K]^T \in \mathbb{R}^K$ is the vector of path gains and $\boldsymbol{\psi} = [\psi_1, \psi_2, \ldots, \psi_K]^T \in \mathbb{R}^K$. We assume that $\boldsymbol{h}$ is Gaussian distributed, namely $\boldsymbol{h} \sim \mathcal{CN}(\boldsymbol{\mu_h}, \boldsymbol{\Sigma_h})$. Then, the source-domain channel response matrix $\boldsymbol{H}^{(\mathsf{s})} \in \mathbb{C}^{N_r \times K}$ can be represented as

$$\left[\boldsymbol{H}^{(\mathsf{s})}\right]_{:,k} = \alpha_k e^{j\psi_k} \cdot \left[1, \ldots, e^{j\frac{2\pi d_s}{\lambda}(N_r-1)\sin(\theta_k)}\right]^T, \quad (2)$$

where $[\cdot]_{:,k}$ means the elements of the kth column in the matrix and the superscript 'T' means the transpose of vector or matrix. Moreover, following the literature [14], [15], the channel gains and AoAs are assumed to be independent of each other.

Based on the "basic" model, the source-domain received signals during the T snapshots, denoted by $\boldsymbol{Y}^{(\mathsf{s})} \in \mathbb{C}^{N_r \times T}$, can be written as

$$\boldsymbol{Y}^{(\mathsf{s})} = \boldsymbol{H}^{(\mathsf{s})}\boldsymbol{X}^{(\mathsf{s})} + \boldsymbol{W}, \quad (3)$$

where $\boldsymbol{X}^{(\mathsf{s})} = \left[\boldsymbol{x}_1^{(\mathsf{s})}, \boldsymbol{x}_2^{(\mathsf{s})}, \ldots, \boldsymbol{x}_T^{(\mathsf{s})}\right] \in \mathbb{C}^{K \times T}$ collects the K transmitted signals respectively from the K MSs, and $\boldsymbol{W} = [\boldsymbol{\omega}_1, \boldsymbol{\omega}_2, \ldots, \boldsymbol{\omega}_T] \in \mathbb{C}^{N_r \times T}$ is the complex circular symmetric white Gaussian noise with $\boldsymbol{\omega}_t \sim \mathcal{CN}(\boldsymbol{0}, \sigma^2\boldsymbol{I}_{N_r})$ for $t = 1, \ldots, T$.

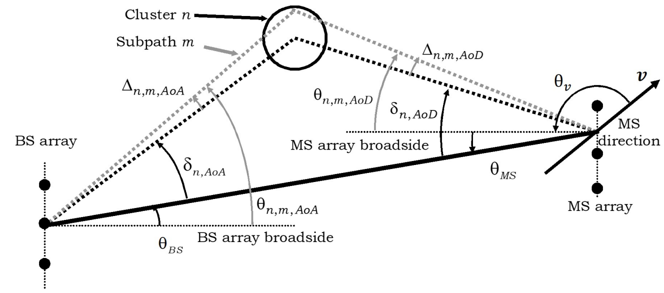

Fig. 1: Illustration of the SCM for urban micro-cell environments with LoS path.

For the target domain, the signal propagation model can be modeled as the SCM for urban micro-cell environments with one BS and K MSs. The BS is still equipped with a ULA of N_r antennas, while each MS equipment has N_t ULA antennas. The channel between each MS and the BS is depicted in Fig. 1. We assume that the SCM consists of N path clusters, including line-of-sight (LoS) path. For each path cluster, there are M sub-paths with the offset AoAs $\Delta_{n,m,AoA}$ and angle-of-departures (AoDs) $\Delta_{n,m,AoD}$, whose values are taken from [13]. The AoA for the LoS component θ_{BS} is defined as the angle between the LoS path direction and the array broadside, so is the AoD for the LoS component θ_{MS}. The N AoDs (in degrees) are independent identically distributed (i.i.d.) uniform random variables $\delta_{n,AoD} \sim U(-40, 40)$, $n = 1, \ldots, N$, while the associated N AoAs (in degrees) are i.i.d. Gaussian random variables $\delta_{n,AoA} \sim \mathcal{N}(0, \sigma_{n,AoA}^2)$, where $\sigma_{n,AoA} = 104.12(1 - e^{-0.265|10\ln(P_n)|})$ and P_n is the relative power of the nth path cluster. The power of each path cluster can be expressed as $P_n^{'} = 10^{-(\tau_n + z_n/10)}$, where $\tau_n \sim U(0, 1.2)$ is the random delays (in microseconds) and $z_n \sim \mathcal{N}(0, \sigma_{z_n}^2)$ is a Gaussian random variable with $\sigma_{z_n} = 3dB$. Thus the relative power is given by

$$P_n = \frac{P_n^{'}}{(\rho+1)\sum_{n=1}^{N} P_n^{'}}, \quad (4)$$

where $\rho = 13 - 0.03d$ is the power ratio of LoS to the scattered paths in dB [16], and d is the distance between MS and BS in meters. Note that the mobility of each MS (with velocity vector $\boldsymbol{v}$ shown in Fig. 1) is also taken into consideration in the target domain.

Thus, for the target domain, the $N_r \times N_t$ channel response matrix can be denoted as

$$\left[\boldsymbol{H}_n^{(\mathsf{t})}(t)\right]_{i,l} = \sqrt{\frac{1}{\rho+1}}\left[\boldsymbol{H}_n(t)\right]_{i,l} \quad (5)$$
$$+ \mathbb{I}(n=1)\sqrt{\frac{\rho\sigma_{SF}^2}{\rho+1}}\left(\begin{array}{c} \sqrt{G_{BS}(\theta_{BS})}e^{j\frac{2\pi d_s(i-1)}{\lambda}\sin(\theta_{\mathrm{BS}})}\times \\ \sqrt{G_{MS}(\theta_{MS})}e^{j\frac{2\pi d_u(l-1)}{\lambda}\sin(\theta_{\mathrm{MS}})}\times \\ e^{j\frac{2\pi}{\lambda}\|\boldsymbol{v}\|\cos((\theta_{\mathrm{MS}}-\theta_{\mathrm{v}})\mathrm{t})}e^{j\phi_{LoS}} \end{array}\right),$$

where $\mathbb{I}(n=1)$ is the indicator function (taking value of $n=1$ (LoS path) and zero otherwise), $\boldsymbol{v} = \|\boldsymbol{v}\|e^{j\theta_v}$ is the velocity of the MS, σ_{SF} ($4dB$) is the log-normal shadowing standard deviation, d_s (d_u) is the inter-element distance of BS (MS) antenna array, and

$$[\boldsymbol{H}_n(t)]_{i,l} = \sqrt{\frac{P_n \sigma_{SF}}{M}} \cdot \sum_{m=1}^{M} \left(\begin{array}{l} \sqrt{G_{BS}(\theta_{n,m,AoA})} e^{j\frac{2\pi d_s (i-1)}{\lambda}\sin(\theta_{\rm n,m,AoA})} \times \\ \sqrt{G_{MS}(\theta_{n,m,AoD})} e^{j\frac{2\pi d_u (l-1)}{\lambda}\sin(\theta_{\rm n,m,AoD})} \times \\ e^{j\frac{2\pi}{\lambda}\|\boldsymbol{v}\|\cos((\theta_{\rm n,m,AoD}-\theta_{\rm v})t)} e^{j\phi_{n,m}} \end{array} \right), \tag{6}$$

where $\phi_{n,m}$ is the angle of the mth sub-path in the path-cluster n. For each and every antenna element at the MS, the antenna pattern is assumed omnidirectional with an antenna gain of -1 dBi, i.e., $G_{MS}(\theta) = 1$. While for each and every antenna element at the BS, the 6-sector antenna pattern is used

$$G_{BS}(\theta) = 10^{-0.1\cdot\left(\min\left[12\left(\frac{\theta}{\theta_{\rm 3dB}}\right)^2, {\rm A_m}\right]\right)}. \tag{7}$$

where $\theta_{3dB} = 35°$ and $A_m = 20dB$.

Based on the SCM, the target-domain received signals are $\boldsymbol{Y}^{(\mathrm{t})} = \left[\boldsymbol{y}^{(\mathrm{t})}(1), \boldsymbol{y}^{(\mathrm{t})}(2), \ldots, \boldsymbol{y}^{(\mathrm{t})}(T)\right] \in \mathbb{C}^{N_r \times T}$, where

$$\boldsymbol{y}^{(\mathrm{t})}(t) = \sum_{n=1}^{N} \boldsymbol{H}_n^{(\mathrm{t})}(t)\boldsymbol{x}_n^{(\mathrm{t})}(t-\tau_n) + \boldsymbol{\omega}_t, \tag{8}$$

in which $\boldsymbol{x}_n^{(\mathrm{t})}(t) \in \mathbb{C}^{N_t}$ is the transmitted signal in the nth path from the MS, and $\boldsymbol{\omega}_t$ is the Gaussian noise defined above.

Let us conclude this section with some notes about the received signals given by (3) in the source domain and that (8) in the target domain as follows. Since each MS has only one antenna $N_t = 1$ and multiple path clusters are not considered for the former, the transmitted signal from all K MSs can be expressed as a matrix $\boldsymbol{X}^{(\mathrm{s})} \in \mathbb{C}^{K\times T}$ in (3), while the transmitted signal in (8) applies to each of the K MSs.

III. Transfer Learning-Based AoAs Estimation Framework

The aim of this paper is to estimate the AoA for the direct component θ_{BS} of each MS, based on the received signals $\boldsymbol{Y}^{(\mathrm{t})}$ in the target domain. Note that the target domain channel response matrix changes due to the different nature of each MS, e.g., the number of antennas N_t, the mobility $\boldsymbol{v}$, etc. The proposed framework allows the designed network to adapt itself to different scenarios AoAs estimation. Next, an overview of our framework and high-level design principles are provided, then followed by presentation in detail.

A. Overview and Design Principles

In the proposed framework, the autocorrelation matrix of the received signals are used as the inputs of the network, which are defined as

$$\begin{cases} \boldsymbol{R}_{\boldsymbol{YY}}^{(\mathrm{s})} = \mathbb{E}\left[\boldsymbol{Y}^{(\mathrm{s})}(\boldsymbol{Y}^{(\mathrm{s})})^H\right] \\ \boldsymbol{R}_{\boldsymbol{YY}}^{(\mathrm{t})} = \mathbb{E}\left[\boldsymbol{Y}^{(\mathrm{t})}(\boldsymbol{Y}^{(\mathrm{t})})^H\right] \end{cases}, \tag{9}$$

where the superscript 'H' means the conjugate transpose. According to [17], the source/target domain can be defined as $\mathcal{D}^{(*)} = \left\{\mathcal{R}_{\boldsymbol{YY}}^{(*)}, P(\boldsymbol{R}_{\boldsymbol{YY}}^{(*)})\right\}$, where $\mathcal{R}_{\boldsymbol{YY}}^{(*)}$ denotes the feature space and $P(\boldsymbol{R}_{\boldsymbol{YY}}^{(*)})$ is the marginal probability density function with $\boldsymbol{R}_{\boldsymbol{YY}}^{(*)} \in \mathcal{R}_{\boldsymbol{YY}}^{(*)}$. Correspondingly, the goal of the proposed transfer learning framework is to come up with the set by $\mathcal{T} \triangleq \left\{\boldsymbol{\Theta}, P(\boldsymbol{\theta}|\boldsymbol{R}_{\boldsymbol{YY}}^{(*)})\right\}$, where $\boldsymbol{\Theta}$ denotes the label space and $P(\boldsymbol{\theta}|\boldsymbol{R}_{\boldsymbol{YY}}^{(*)})$ is the posterior probability density function with $\boldsymbol{\theta} \in \boldsymbol{\Theta}$.

As presented in Section II, let us emphasize that the AoA (θ_k) for MS k at the BS for the source model is actually the same as θ_{BS} (LoS path angle) for the target model for MS k, thereby disclosing some common features (through their array response vectors) shared by the two channel models. Therefore, we come up with an important conjecture that both domains share some common features for AoAs estimation, thereby providing the assumption for the design of the proposed framework and its validity to be justified by experimental results later.

As a result, a canonical approach of transfer learning is considered that uses some layers to learn the common features of both domains while the other layers are used to extract other features. Thus, the proposed framework can be divided into transfer layers (TL) and fine-tuning layers (FL). The former is used to learn the common features of both domains, while the latter is used to extract the other characteristic features.

Mathematically, we can model the TL as a function $g_{\boldsymbol{\theta}}^{TL}(\cdot)$, and the FL as $g_{\boldsymbol{\theta}^{(\mathrm{s})}}^{FL}(\cdot)$ and $g_{\boldsymbol{\theta}^{(\mathrm{t})}}^{FL}(\cdot)$ for source-domain and target-domain AoAs estimation, respectively. On this base, the common features of both domain channels can be extracted via $g_{\boldsymbol{\theta}}^{TL}(\boldsymbol{R}_{\boldsymbol{YY}}^{(*)})$ and fed into the FL. As a result, the network parameters estimation of the target domain can be composedly expressed as

$$\widehat{\boldsymbol{\theta}}^{(\mathrm{t})} = g_{\boldsymbol{\theta}^{(\mathrm{t})}}^{FL}(g_{\boldsymbol{\theta}}^{TL}(\boldsymbol{R}_{\boldsymbol{YY}}^{(\mathrm{t})})). \tag{10}$$

In order to make sure that $\widehat{\boldsymbol{\theta}}^{(\mathrm{t})} \to \boldsymbol{\theta}^{(\mathrm{t})}$, where "$\to$" means "approaches to", the weights of the proposed framework should be updated so as to achieve $g_{\boldsymbol{\theta}^{(\mathrm{t})}}^{FL}(g_{\boldsymbol{\theta}}^{TL}(\boldsymbol{R}_{\boldsymbol{YY}}^{(\mathrm{t})})) \to P^*(\boldsymbol{\theta}|\boldsymbol{R}_{\boldsymbol{YY}}^{(\mathrm{t})})$, where $P^*(\boldsymbol{\theta}|\boldsymbol{R}_{\boldsymbol{YY}}^{(\mathrm{t})})$ is the optimal posterior probability density function.

B. Implementation of Proposed Framework

Figure 2 shows a detailed architecture flowchart of the proposed transfer learning framework, where a deep residual network-18 (ResNet-18) is used as its backbone. The TL consists of residual connection blocks of the ResNet, while the FL consists of fully connected layers. In order to reduce the possibility of overfitting in the source domain and to smoothly operate in the target domain, a dropout layer is inserted into each of two layers in FL.

In the proposed framework, the number of labeled training data in the source domain is assumed ten times that in the target domain. To be addressed in Section III, training the specific network for each channel with limited training data is difficult. Hence, it is important to pre-train the proposed framework with labeled training data in the source domain. In the pre-training phase, the data in the source domain is

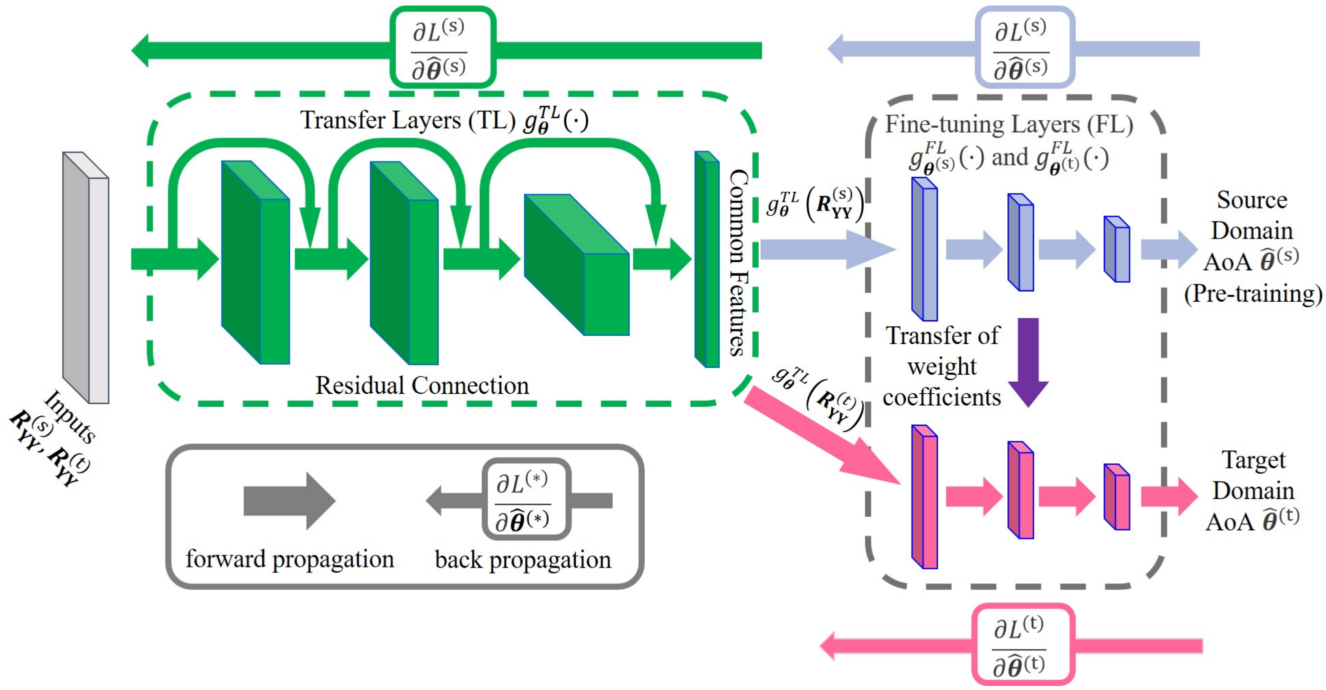

Fig. 2: Illustration of the proposed transfer learning framework.

divided into training data and validation data, and the output $\widehat{\boldsymbol{\theta}}^{(s)}$ is used to evaluate the pre-training of the network. Thus, the weights of the network is updated to minimize the loss function as follows:

$$L^{(s)} = \mathbb{E}\left[\|\boldsymbol{\theta}^{(s)} - \widehat{\boldsymbol{\theta}}^{(s)}\|_2^2\right], \tag{11}$$

where $\|\cdot\|_2$ stands for ℓ_2-norm of vectors and the network is evaluated by the validation data.

Since the channel model and the marginal distribution of the data are different for each of the two domains, the pre-trained network cannot be used directly in the target domain. It is necessary to fine-tune the weights of the network by a few labeled training data in the target domain for the domain adaptation. In the proposed framework, since the TL is to extract the common features of both domains, the weights of TL are fixed after the pre-training. Thus, we fine-tune the weights of the FL with a few labeled training data in the target domain with a fine-tuning loss function as follows:

$$L^{(t)} = \mathbb{E}\left[\|\boldsymbol{\theta}^{(t)} - \widehat{\boldsymbol{\theta}}^{(t)}\|_2^2\right]. \tag{12}$$

IV. Numerical Simulations

In this section, we evaluate the performance of the proposed framework and compare with some benchmark methods. Different scenarios such as the mobility, the antenna array configuration, will be taken into consideration to demonstrate the high domain adaptability of the proposed framework. We compare the estimation accuracy of the proposed framework with the canonical MUSIC algorithm [1] and the supervised DL-based estimation method. The architecture of the latter is also used in the proposed framework. In order to extract the latent information of the sophisticated channel in the target domain, the residual connections are considered to build a deep network without vanishing/exploding gradient, i.e., ResNet-18. The performances of the proposed framework in the following figure will be marked as "Ours", together with those of the MUSIC algorithm as "MUSIC" and the supervised DL-based estimation method as "Supervised".

We set the number of MSs $K = 2$, the number of snapshots $T = 32$, the number of BS antennas $N_r = 32$, the number of MS antennas $N_t = 1$ and the antenna spacing for both BS and MS as $d_s = d_u = \lambda/2$, unless clearly re-specified. The neural network is trained by the adaptive moment estimation algorithm with a fixed learning rate of 10^{-4}. The batch size of the input data is 128. The source-domain training data set includes 40960 samples and the validation data set has 10240 samples, while in the target domain, there are 5120 samples for both labeled fine-tuning data set and unlabeled test data set. The maximum number of the pre-training epochs is set to 100 while that for the fine-tuning phase is set to 50, and the network is trained for SNR values between $0dB$ and $20dB$ separately

A. Performance Comparison

We first evaluate the performance of the proposed framework, for which all the parameters of the SCM in the target domain are the same as those of the "basic" channel in the source domain.

Figure 3 shows the mean squared error (MSE) of the AoAs estimation in the target domain. It can be seen from this figure that all the methods under test perform better for fewer MSs, and the MUSIC performs best for the case of one MS. The

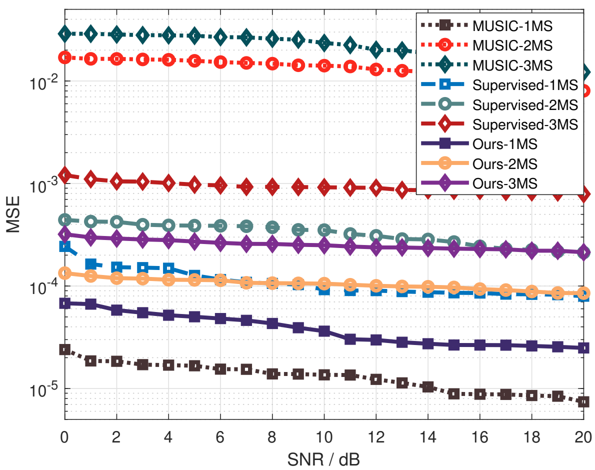

Fig. 3: Performance (MSE versus SNR) comparison of the proposed framework, the MUSIC algorithm and the supervised learning method, with SNRs of the received signals following the uniform distribution $U(0, 20)$ in dB used in the pre-training, and all the MSs assumed stationary.

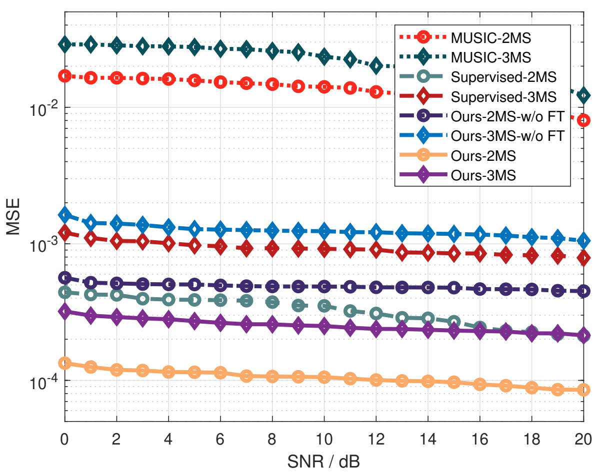

Fig. 4: Performance (MSE versus SNR) comparison of the proposed framework (for which "w/o FT" means "without the fine-tuning phase"), the MUSIC algorithm and the supervised learning method.

MUSIC, in spite of the best performance for the single MS case, performs significantly worse than both the supervised DL-based method and the proposed framework due to the non-ignorable cross channel correlation and interference between MSs. These results also demonstrate the best performance of the proposed framework, including its higher robustness to the number of MSs.

To show the impact of the-tuning layers on the performance of the proposed framework, some simulation results are shown in Fig. 4. Again, as observed from Fig. 3, all the methods under test perform better for fewer MSs. An interesting observation, from Fig. 4, is that the performance of the proposed framework without applying the fine-tuning is somewhat worse than that of the supervised DL-based method; however, the former is significantly better than the latter when the fine-tuning layers is applied in the target domain. Therefore, these results also show the powerfulness of the fine-tuning in the extraction of the common feature in both domains, thereby enabling the proposed framework to well learn in-depth channel information in addition to robust domain adaptability.

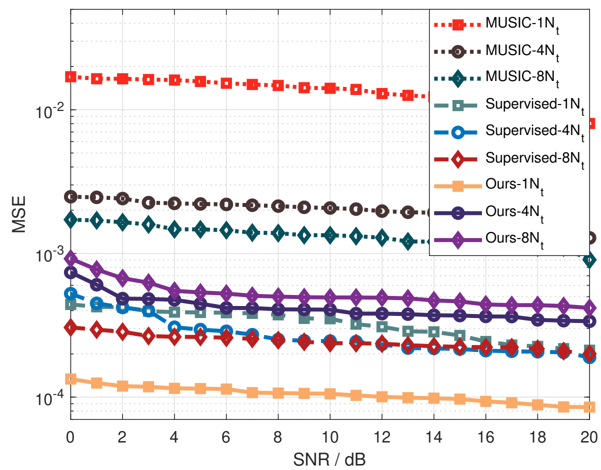

Fig. 5: Performance (MSE versus SNR) comparison of the proposed framework, the MUSIC algorithm and the supervised learning method for the number of ULA antennas $N_t \in \{1, 4, 8\}$ of each MS.

B. Performance Sensitivity Evaluation

Because of the slow fading channel assumed in the source domain and the target domain, the performance of the proposed method is insensitive to T (the number of snapshots), we only show some simulation results on the performance sensitivity of the proposed method to N_t (number of antenna elements of each MS) and the mobility of MSs.

1) Number of Antennas N_t: It is obvious to see, from (2) and (5), that the target-domain channel is very different from the source-domain channel because of the mismatch of AoAs and AoDs in the SCM.

Figure 5 shows that the MUSIC method and the supervised DL-based method perform better for larger N_t thanks to larger diversity gain. However, the mismatch of AoAs and AoDs implies that the SCM becomes more complicated for larger N_t, thus leading to some performance degradation. Nevertheless, the performance of the proposed framework is still comparable to the supervised DL-based method.

2) Mobility: It can be seen from (5) that the channel response matrix (the target domain) is also dependent upon the mobility of the MS, thus having impact on the performance. Next, we show some simulation results for all the methods

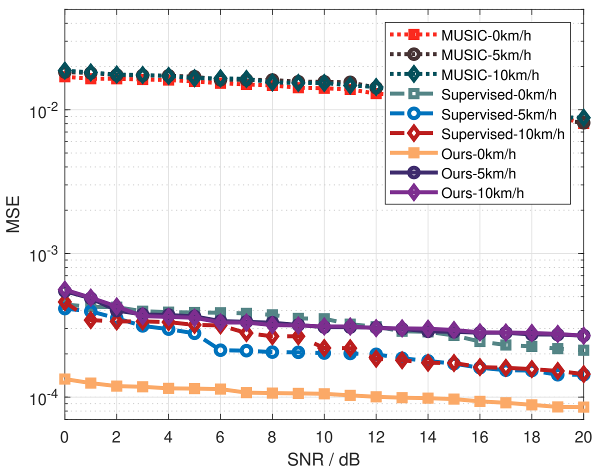

Fig. 6: Performance (MSE versus SNR) comparison of the proposed framework, the MUSIC algorithm and the supervised learning method for mobile speeds $\|\boldsymbol{v}\| \in \{0, 5, 10\}$ (km/h).

under test only under the low mobility scenario, since they all fail under the high mobility scenario.

Figure 6 shows the performance simulation results for the mobile MS with speed $\|\boldsymbol{v}\| \in \{0, 5, 10\}$ (km/h). One can see from this figure that the MUSIC method and the supervised DL-based method are less sensitive to the mobility of the MS than the proposed framework. The reason for this may be that the mobility of the MS is not considered in the source domain. Nevertheless, the performances of the proposed framework and the supervised DL-based method are still quite comparable, and the former performs remarkably better than the latter when the MS is not mobile, thus demonstrating its good domain adaptability under the low mobility scenario.

V. Conclusions

We have presented a TL framework (cf. Fig. 2) for AoAs estimation by simultaneously considering different channel models in massive MIMO systems, thus providing a solution to the computational bottleneck of DL-based methods, i.e., training a specific network for each channel with limited labeled data. The proposed framework is composed of TL layers and FL layers in cascade, where the former (the latter) is to extract the common feature of channels in the source domain (other channel characteristics in the target domain) for accurate AoAs estimation in both domains. Therefore, the proposed framework is also a more practical application of the prospective TL in AoAs estimation than existing DL-based methods. Some numerical simulations were also presented to demonstrate the effectiveness of the proposed framework with mean square error performance comparable to DL-based methods.

Some further studies are left in the future, including 1) qualitative and/or quantitative analyses of the convergence analysis of the proposed TL based method for AoAs estimation, and 2) its applications in various wireless communication scenarios and applications.

References

[1] P. Stoica and A. Nehorai, "MUSIC, maximum likelihood and Cramer-Rao bound: Further results and comparisons," in *Proc. International Conference on Acoustics, Speech, and Signal Processing*, 1989, pp. 2605–2608.
[2] R. Roy and T. Kailath, "Esprit-estimation of signal parameters via rotational invariance techniques," *IEEE Transactions on Acoustics, Speech, and Signal Processing*, vol. 37, no. 7, pp. 984–995, 1989.
[3] D. Fan, G. Guo, J. Song, L. Li, and Y. Zhu, "DOA estimation for arbitrarily distributed subarrays in UAV swarm," in *2020 IEEE/CIC International Conference on Communications in China (ICCC)*, 2020, pp. 794–799.
[4] H. He, Y. Liang, and S. Li, "Clustering algorithm based on azimuth in mmwave massive MIMO-NOMA system," in *Proc. 2021 IEEE/CIC International Conference on Communications in China (ICCC Workshops)*, 2021, pp. 118–122.
[5] Y. Wang, Y. Zhang, Z. Tian, G. Leus, and G. Zhang, "Super-resolution channel estimation for arbitrary arrays in hybrid millimeter-wave massive MIMO systems," *IEEE Journal of Selected Topics in Signal Processing*, vol. 13, no. 5, pp. 947–960, 2019.
[6] M. Wagner, Y. Park, and P. Gerstoft, "Gridless DOA estimation and root-MUSIC for non-uniform linear arrays," *IEEE Transactions on Signal Processing*, vol. 69, pp. 2144–2157, 2021.
[7] Z. Qin, H. Ye, G. Y. Li, and B.-H. F. Juang, "Deep learning in physical layer communications," *IEEE Wireless Communications*, vol. 26, no. 2, pp. 93–99, 2019.
[8] H. He, S. Jin, C.-K. Wen, F. Gao, G. Y. Li, and Z. Xu, "Model-driven deep learning for physical layer communications," *IEEE Wireless Communications*, vol. 26, no. 5, pp. 77–83, 2019.
[9] H. Huang, J. Yang, H. Huang, Y. Song, and G. Gui, "Deep learning for super-resolution channel estimation and DOA estimation based massive MIMO system," *IEEE Transactions on Vehicular Technology*, vol. 67, no. 9, pp. 8549–8560, 2018.
[10] A. Barthelme and W. Utschick, "DoA estimation using neural network-based covariance matrix reconstruction," *IEEE Signal Processing Letters*, vol. 28, pp. 783–787, 2021.
[11] Y. Yang, N. Zou, E. Lin, F. Suo, and Z. Chen, "A neural network method for nonconvex optimization and its application on parameter retrieval," *IEEE Transactions on Signal Processing*, vol. 69, pp. 3383–3398, 2021.
[12] C. Liu, Z. Wei, D. W. K. Ng, J. Yuan, and Y.-C. Liang, "Deep transfer learning for signal detection in ambient backscatter communications," *IEEE Transactions on Wireless Communications*, vol. 20, no. 3, pp. 1624–1638, 2021.
[13] 3GPP TR 25.996 V16.0.0, "Spatial channel model for multiple input multiple output (MIMO) simulations," *3rd Generation Partnership Project (3GPP)*, 2020.
[14] M.-A. Badiu, T. L. Hansen, and B. H. Fleury, "Variational Bayesian inference of line spectra," *IEEE Transactions on Signal Processing*, vol. 65, no. 9, pp. 2247–2261, 2017.
[15] T. L. Hansen, B. H. Fleury, and B. D. Rao, "Superfast line spectral estimation," *IEEE Transactions on Signal Processing*, vol. 66, no. 10, pp. 2511–2526, 2018.
[16] H. Foster, S. Dehghan, R. Steele, J. Stefanov, and H. Strelouhov, "Microcellular measurements and their prediction," in *IEE Colloquium on Role of Site Shielding in Prediction Models for Urban Radiowave Propagation (Digest No. 1994/231)*, 1994, pp. 2/1–2/6.
[17] F. Zhuang, Z. Qi, K. Duan, D. Xi, Y. Zhu, H. Zhu, H. Xiong, and Q. He, "A comprehensive survey on transfer learning," *Proceedings of the IEEE*, vol. 109, no. 1, pp. 43–76, 2021.